Swing-Up of Underactuated Compliant Arms via Iterative Learning Control

Michele Pierallini, Franco Angelini, Antonio Bicchi, and Manolo Garabini

***Abstract*—The swing-up is a classical problem of control theory that has already been widely studied in the literature. Despite that, swinging up an underactuated compliant arm considerably increases the problem complexity. Indeed, in addition to the problem of underactuation, compliant systems usually present also hard-to-model dynamics. Moreover, the control authority of feedback components should be limited to avoid radical alteration of the robot natural elasticity. In this letter, we tackle the swing-up problem of underactuated compliant arms via an Iterative Learning Control approach, proving its convergence. The proposed control law combines feedforward and feedback terms. Tracking the desired trajectory, i.e., bringing the robot up to its vertical equilibrium, is achieved thanks to the feedforward components. Conversely, the feedback of the output signal is used to stabilize the system at the equilibrium point. Additionally, we study the stiffness variation caused by the employed feedback, deriving a condition to preserve the elasticity of the compliant arm. Finally, we validate the proposed method via simulations and experiments underactuated compliant arms with unstable vertical equilibrium varying number of unactuated joints, payload, stiffness, model uncertainties, and noise.**

***Index Terms*—Flexible Robotics; Underactuated Robots; Modeling, Control, and Learning for Soft Robots**

I. Introduction

SWINGING up an underactuated system has always been one of the most fascinating problems in robotics [1]. Two main challenges of this task are two: tracking the desired trajectory to reach the vertical position and stabilizing the system in this (unstable) equilibrium. Given the different nature of these two problems, a solution is the employment of two different controllers. In [1], the Author introduces the famous partial feedback linearization to swing the robot up, and then, the system is stabilized via a Linear Quadratic Regulator. Other solutions employ Lyapunov-based controllers [2], optimal policies [3], or model predictive control [4]. However, these controllers require a reliable model description and/or (high gain) feedback components. Lately, the advent of learning-based and model-free techniques introduces novel solutions for the swing-up task, for instance, fuzzy controllers [5], genetic algorithms [6], and reinforcement learning [7].

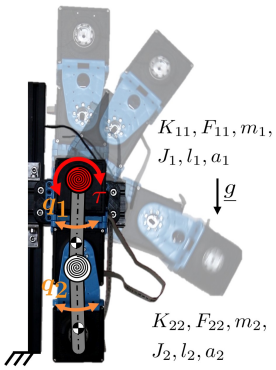

Fig. 1. Underactuated complaint arm performing a swing-up motion. The system presents two elastic joints, the base one (red) is actuated, while the second one (white) is unactuated.

In this work, we focus on the swing-up problem of underactuated compliant arms. These systems belong to the class of soft robots [8], [9], since they present elastic elements into their structure. Controlling soft robots introduces novel additional challenges: their dynamics is usually complex [10], thus its model description is typically not reliable. Moreover, high gain feedback controllers hinder the natural compliance of the system [11], [12]. For these reasons, the applicability of classical model-based control approaches with high-gain feedback terms is not recommended. On the other hand, learning-based methods promise to be a valid alternative, because they can be designed as mostly feedforward [13] avoiding any substantial change in the robot dynamics [14]. However, these policies are time-consuming, and they typically miss a formal study of the intrinsic properties of the system, e.g., stability [15].

Iterative Learning Control (ILC) approaches [16] are able to solve these issues. On the one hand, ILC improves the tracking performance by exploiting the previous iteration tracking error without requiring any accurate robot modeling. Furthermore, it preserves the system compliance, because it mainly relies on feedforward components. On the other hand, using ILC we can draw formal conclusions on the stability of the vertical equilibrium and on the iterative procedure convergence. ILC has already been applied to articulated soft robots, e.g., [12], [17], [18], however, the swing-up problem with underactuated compliant arms is still open.

In this letter, we solve the swing-up problem for underactuated compliant arms. We propose an ILC law for a class of nonlinear systems with an arbitrary fixed relative degree,

Manuscript received September 09, 2021; revised November 12, 2021; accepted January 01, 2022.

This paper was recommended for publication by Editor C. Gosselin upon evaluation of Reviewers' comments. This work was supported by the European Union's Horizon 2020 Research and Innovation Programme under Grant Agreement No. 101016970 (Natural Intelligence), No. 871237 (SOPHIA), and No. 779963 (EUROBENCH) as funded project DYSTURBANCE. (*Corresponding Author: Michele Pierallini*).

Michele Pierallini, Franco Angelini, Antonio Bicchi, and Manolo Garabini are with the Centro di Ricerca "Enrico Piaggio" and the Dipartimento di Ingegneria dell'Informazione, Università di Pisa, Largo Lucio Lazzarino 1, 56126 Pisa, Italy (e-mail: {michele.pierallini, frncangelini, manolo.garabini}@gmail.com).

Antonio Bicchi is with the Soft Robotics for Human Cooperation and Rehabilitation, Fondazione Istituto Italiano di Tecnologia, via Morego, 30, 16163 Genova, Italy (e-mail: antonio.bicchi@unipi.it).

This articles has supplementary downloadable materials available at IEEE.

Digital Object Identifier (DOI): see top of this page.

proving its convergence. The proposed algorithm combines feedforward and feedback terms. The former is used to track the desired trajectory, while the latter is an output feedback regulator, which stabilizes the robot vertical equilibrium through the application of the Lyapunov indirect Theorem. To preserve the robot elastic behavior, we propose a condition, which bounds the distance between open and closed-loop stiffness. A procedure to select the control gains guarantee the convergence is also presented. Finally, we validate the proposed approach in both simulations and on real hardware executing a swing-up task with underactuated compliant arms presenting unstable vertical equilibrium. We simulate the dynamics of a two and a three Degrees of Freedom (DoFs) robot varying model uncertainties, noise, and control action at the first iteration - namely initial guess. In the experiments, the employed testbed is a two DoFs robot, in which only the first elastic joint is actuated (Fig. 1). Furthermore, we vary the payload and the joint stiffness.

Notation: Let $1_{1\times n} = [1,\cdots,1] \in \mathbb{R}^{1\times n}$, $I_n \in \mathbb{R}^{n\times n}$ be the identity matrix, and $0_{n\times m} \in \mathbb{R}^{n\times m}$ be a zero matrix. Let $f,g : x \in \mathbb{R}^n \to \mathbb{R}^n$ be two vector fields, $L_f g(x)$ stands for the Lie derivative of $g(x)$ along $f(x)$, i.e., $L_f g(x) = \frac{\partial g(x)}{\partial x} f(x)$. For any vector $v \in \mathbb{R}^n$, for any matrix $A \in \mathbb{R}^{n\times m}$, we denote with $||v||$ and $||A||$ their infinity norm. For any matrix $A \in \mathbb{R}^{n\times m}$, the symbol $A_{i,s}$ indicates its $is-$th element $i = 1,\cdots,n$ and $j = 1,\cdots,m$. Let be $\lambda > 0$, for any vector $v \in \mathbb{R}^n$, we denote with $||v||_\lambda$ its $\lambda-$norm, i.e., $||v||_\lambda \triangleq \sup_t \left\{||v||\, e^{-\lambda t}\right\}$. Let $y : t \in \mathbb{R} \to \mathbb{R}^n$ be a vector function, $y^{(i)}(t)$ stands for its $i-$th time derivative. Finally, we specify the positive definiteness of any matrix $A \in \mathbb{R}^{n\times n}$ as $A \succ 0$.

II. Problem Definition and Preliminaries

Let us consider the model of a $n-$DoFs underactuated compliant arms, i.e.,

$$M(q)\ddot{q} + C(q,\dot{q})\dot{q} + G(q) + F\dot{q} + Kq = S\tau + \tau_{\text{ext}}, \qquad (1)$$

where $q,\dot{q},\ddot{q} \in \mathbb{R}^n$ are the position, velocity and acceleration vectors, respectively. $M(q) \in \mathbb{R}^{n\times n}$ is the inertia matrix of the robot, which is symmetric and $M(q) \succ 0$, $C(q,\dot{q}) \in \mathbb{R}^{n\times n}$ includes Coriolis terms, $G(q) \in \mathbb{R}^n$ is the gravity vector, and $F,K \in \mathbb{R}^{n\times n}$ are the diagonal damping and stiffness matrix such as $F,K \succ 0$, respectively. The underactuation matrix $S \in \mathbb{R}^{n\times m}$ maps the input to the dynamics of all the robot joints and $\text{rank}\{S\} = m < n$ and $\tau \in \mathbb{R}^m$ is the torque control input. Finally, the vector $\tau_{\text{ext}} \in \mathbb{R}^n$ collects the external torque.

Let us consider an iterative process with iteration index $j \in \mathbb{N}_0$. We follow the classic affine state-space form defining the state $x_j \triangleq \left[q_j^\top,\ \dot{q}_j^\top\right]^\top \in \mathbb{R}^{2n}$ for continuous time systems. Hence, the system (1) can be written as

$$\begin{cases} \dot{x}_j(t) = f(x_j(t)) + g(x_j(t))u_j(t) + v_j(t) & (2) \\ y_j(t) = h(x_j(t)) + w_j(t)\,, & (3) \end{cases}$$

with $x_j(0) \in \mathbb{R}^{2n}$ as initial condition, $t \in [0,t_{\text{f}}]$ is the time variable (t_{f} terminal time), and $u_j(t) \in \mathbb{R}^m$ is the control input, i.e., τ. $y_j(t) \in \mathbb{R}^{n_{\text{y}}}$ is the output, $h(\cdot) : \mathbb{R}^{2n} \times [0,t_{\text{f}}] \to \mathbb{R}^{n_{\text{y}}}$ is the output function, $f(\cdot) : \mathbb{R}^{2n} \times [0,t_{\text{f}}] \to \mathbb{R}^n$, $g(\cdot) : \mathbb{R}^{2n} \times [0,t_{\text{f}}] \to \mathbb{R}^{2n\times m}$ are the drift and control vector fields

$$f(x_j) = \begin{bmatrix} \dot{q}_j \\ -M^{-1}(q_j)N(q_j,\dot{q}_j) \end{bmatrix},\ g(x_j) = \begin{bmatrix} 0_{n\times m} \\ M^{-1}(q_j)S \end{bmatrix}, \qquad (4)$$

with $N(q_j,\dot{q}_j) \triangleq C(q_j,\dot{q}_j)\dot{q}_j + G(q_j) + Kq_j + F\dot{q}_j$. The disturbances are $v_j(t) : [0,t_{\text{f}}] \to \mathbb{R}^{2n}$, which may include τ_{ext}, and $w_j(t) : [0,t_{\text{f}}] \to \mathbb{R}^{n_{\text{y}}}$ is the measurement noise.

Let $y_{\text{d}}(t) : [0,t_{\text{f}}] \to \mathbb{R}^{n_{\text{y}}}$ be the desired trajectory to follow, the following definition is instrumental to ensure the existence of the control problem solution.

Definition 1. *The desired trajectory $y_{\text{d}}(t) : [0,t_{\text{f}}] \to \mathbb{R}^{n_{\text{y}}}$ is said to be feasible when there exist $u_{\text{d}} \in \mathbb{R}^m$ and $x_{\text{d}} \in \mathbb{R}^{2n}$, which are the desired control input and state, such that $\dot{x}_{\text{d}}(t) = f(x_{\text{d}}(t)) + g(x_{\text{d}}(t))u_{\text{d}}(t)$ and $y_{\text{d}}(t) = h(x_{\text{d}}(t))$.*

Recalling the system (2)-(3), the following assumptions are instrumental for the description of the method.

Assumption 1. *The system (2)-(3) is square, i.e., $n_{\text{y}} = m$.*

Assumption 2. *The system (2)-(3) has a fixed vector relative degree r_{v}, $\forall x \in \mathbb{R}^{2n}$ (see, e.g., [19]) $r_{\text{v}} = [r_1,\ldots,r_m]$, i.e.,*

- *$L_{g_i}L_f^k h_s(x) = 0$ with $i,s = 1\ldots m, k = 0\ldots r_{s-1}$.*
- *$\text{rank}\{D(x)\} = m, \forall x \in \mathbb{R}^n$, with $D_{i,s}(x) = L_{g_i}L_f^{r_{s-1}} h_s(x)$.*

Furthermore, we assume that $r = r_1 = \cdots = r_m$.

The matrix $D(x) \in \mathbb{R}^{m\times m}$ is computed such as $D_{i,s}(x) \triangleq L_{g_i}L^{r_{s-1}} h_s(x)$, $\forall i,s = 1\ldots m$ (see, e.g., [19]) and it is commonly called the decoupling matrix of the system (2)-(3).

Assumption 3. *The vector fields $f(\cdot)$, $L_f^i h(\cdot), i = 0,\cdots,r$, $h(\cdot)$, $g(\cdot)$, and $D(\cdot)$ are globally Lipschitz with unknown constants f_0, $\phi_i, i = 0,\cdots,r$, h_0, g_0, and $D_0 \in \mathbb{R}$, respectively, i.e., $||f(\bar{x}_1) - f(\bar{x}_2)|| \le f_0||\bar{x}_1 - \bar{x}_2||$, $\forall \bar{x}_1, \bar{x}_2 \in \mathbb{R}^{2n}$, $f_0 \in \mathbb{R}$.*

Assumption 4. *The desired output trajectory $y_{\text{d}}(t) : [0,t_{\text{f}}] \to \mathbb{R}^m$ is feasible (see Def. 1), continuous, bounded, and differentiable for, at least, r times, $\forall t \in [0,t_{\text{f}}]$.*

Assumption 5. *The non repetitive disturbances in (2)-(3) are bounded, i.e., $\sup_j \left\{\max_t \left\{\left|\left|w_j(t)\right|\right|\right\}\right\} \le b_{\text{w1}}$ and $\sup_j \left\{\max_t \left\{\left|\left|v_j(t)\right|\right|\right\}\right\} \le b_{\text{v}}$, $b_{\text{w1}}, b_{\text{v}} \in \mathbb{R}_+ \setminus \{+\infty\}$. The initial condition $x_j(0) \in \mathbb{R}^{2n}$ presents a bounded shift from the desired one, i.e., $x_j(0) = x_{\text{d}}(0) + l_j$, $l_j \in \mathbb{R}^{2n}, \forall j \in \mathbb{N}_0$, i.e., $\sup_j \left\{\left|\left|l_j\right|\right|\right\} \le b_{\text{l}}$, $b_{\text{l}} \in \mathbb{R}_+ \setminus \{+\infty\}$. Additionally, we assume the output disturbances to be $r-$times time differentiable, with bounded derivatives, i.e., $b_{\text{w2}},\cdots,b_{\text{wr}} \in \mathbb{R}_+ \setminus \{+\infty\}$.*

Consider a system (2)-(3), under assumptions A1-A5. Given the desired output trajectory $y_{\text{d}}(t) : [0,t_{\text{f}}] \to \mathbb{R}^m$, which brings the underactuated compliant arm from the initial position to the equilibrium point $\bar{x} = \left[\bar{q}^\top, 0_{n\times 1}^\top\right]^\top$, the goal of this work is to design an opportune control action combining feedforward and feedback terms $u(\cdot) = u_{\text{fb}}(\cdot) + u_{\text{ff}}(\cdot)$, able to track $y_{\text{d}}(t)$. Other control objectives are listed as follows.

G1) Given a finite constant $\beta \ge 0$, the feedback controller $u_{\text{fb}}(\cdot) \in \mathbb{R}^m$ should not modify the distance between open-loop and closed-loop stiffness more than β, i.e.,

$$\left|\left| \left.\frac{\partial T(q)}{\partial q}\right|_{q=\bar{q}} - \frac{\partial T(q)}{\partial q} - \frac{\partial S u_{\text{fb}}(\cdot)}{\partial q} \right|\right| \le \beta \qquad (5)$$

where $T(q):\mathbb{R}^n\to\mathbb{R}^n$ is the elastic force and $\overline{q}\in\mathbb{R}^n$ is an equilibrium configuration.

G2) The control law should not require an accurate description of the model (2) and it employs only output measurements for the feedback, i.e., $u_{\rm fb}(t,y,\dot{y},\cdots)\in\mathbb{R}^m$.

G3) The feedback controller $u_{\rm fb}(t,y,\dot{y},\cdots)\in\mathbb{R}^m$ is designed in such a way that the equilibrium $\overline{x},\overline{u}$ is asymptotically stable for the system (2).

It is worth noting that Def. 1 and the control objectives do not refer exclusively to swing-up tasks, but they include any trajectories and (unstable) equilibria. Without loss of generality, we focus on the swing-up task, because it is one of the most fascinating problems in robotics and control theory.

III. Problem Solution

To solve the swing-up problem defined in Sec. II, first, we derive a condition aimed to preserve the elasticity of the compliant robot. Then, we design an iterative control law combining feedback and feedforward terms, and we study the stability of the vertical equilibrium. Finally, we wrap everything together proposing a choice of gains to stabilize the system, preserve the elastic behavior, and verify the convergence condition of the iterative control law.

A. Preserve the Elasticity of the Robot

Naive use of feedback control can drastically alter the system compliance [11] and [12]. This effect is undesired and should be avoided whenever possible when controlling compliant robots. However, when studying equilibria stability, a feedback component is usually required. In this case, it is suggested to limit the feedback action to limit the stiffness alteration. This section is intended to analyze the results presented in [11] also for underactuated compliant systems. The main idea is to bound the distance between the open-loop and closed-loop stiffness achieving G1).

Proposition 1. *Let us consider the underactuated compliant system* (1)*, let* $\tau(\cdot)=\tau_{\rm ff}(t)+\tau_{\rm fb}(q,\cdot)$ *be the control action, let* $\tau_{{\rm fb}_i}$ *be the i-th element of* $\tau_{\rm fb}$*, and let* β *be a finite positive constant. If the controller is such that*

$$\max_{i=1,\cdots,m}\left\{\left|\partial\tau_{{\rm fb}_i}(q,\cdot)/\partial q\right|\right\}\leq\beta\,, \tag{6}$$

then the distance between the open-loop and closed-loop stiffness is bounded, i.e., (5) *holds.*

Proof. Recalling (1) and (5), the robot open-loop stiffness can be computed from the elastic force $T(q)$ as $\partial T(q)/\partial q = K\in\mathbb{R}^{n\times n}$. Conversely, the closed-loop stiffness is modified by the feedback controller $\tau_{\rm fb}(q,\cdot)$ such as $K'=\left(K+S\frac{\partial\tau_{\rm fb}(q,\cdot)}{\partial q}\right)$. Then, the distance in (5) is $||K-K'||=||S\partial\tau_{\rm fb}(q,\cdot)/\partial q||$. Recalling the infinity norm definition leads to (6), concluding the proof. □

In (6), $\tau_{\rm fb}(\cdot)$ is the feedback control input, whose design will be studied in the following section, i.e., $\tau(\cdot)=u(\cdot)$.

B. Iterative Learning Control

To solve the swing-up problem, we propose a controller, which belongs to the ILC class [20]. The iterative framework exploits repetitions of the desired task to improve the tracking performance while compensating the uncertainties between the nominal model and the real system.

Recalling the system (2)-(3), we define the following control law combining feedforward and feedback terms as

$$u_{j+1}(t)=\underbrace{u_j(t)+\Gamma_{{\rm ff}_j}(t)\,{}^r e_j(t)}_{u_{{\rm ff}_j}(t)}+\underbrace{\Gamma_{{\rm fb}_{j+1}}(t)\,{}^r e_{j+1}(t)}_{u_{{\rm fb}_{j+1}}(t)}\,, \tag{7}$$

where $\Gamma_{{\rm fb}_{j+1}},\Gamma_{{\rm ff}_j}\in\mathbb{R}^{m\times m}$ are the learning gains which are both time and iteration varying. The error signal ${}^r e_j(t)\in\mathbb{R}^m$ is defined as

$$\begin{aligned}{}^r e_j(t)\triangleq\sum_{i=0}^{r}{}^i\Upsilon\left(y_{\rm d}^{(i)}(t)-y_j^{(i)}(t)\right)=\sum_{i=0}^{r}{}^i\Upsilon w_j^{(i)}(t)+\\ \sum_{i=0}^{r}{}^i\Upsilon\left(L_f^i h(x_{\rm d})-L_f^i h(x_j)\right)+{}^r\Upsilon\left(D(x_{\rm d})u_{\rm d}-D(x_j)u_j(t)\right)\,,\end{aligned} \tag{8}$$

where ${}^i\Upsilon\in\mathbb{R}^{m\times m}$ and ${}^i\Upsilon\succ 0$, for $i=0,\cdots,r$ are the tunable control gains, which affect the convergence velocity [18]. The initial guess $u_0(t)\in\mathbb{R}^m$ can be arbitrarily chosen, and it may rely on a partial knowledge of the model, while the error ${}^r e_0(t)$ is assumed null.

We remark that the system is underactuated, i.e., $m<n$, and usually undersensed, hence a common practice is the output feedback such as in (7).

The following Theorem presents a sufficient convergence condition for the control law (7).

Theorem 1. *Let us consider the system in the form* (2)-(3) *under assumptions A1-A5, and let* (7) *be the iterative control law. If the gains* $\Gamma_{{\rm fb}_{j+1}}(t),\Gamma_{{\rm ff}_j}(t)\in\mathbb{R}^{m\times m}$ *in* (7) *satisfy*

$$\begin{cases}\left|\left|\left(I_m+\Gamma_{{\rm fb}_{j+1}}(t)\,{}^r\Upsilon D(x_{j+1})\right)^{-1}\right|\right|\leq\rho_{\rm fb}<1\\ \left|\left|I_m-\Gamma_{{\rm ff}_j}(t)\,{}^r\Upsilon D(x_j)\right|\right|\leq\rho_{\rm ff}<1\end{cases} \tag{9}$$

$\forall t\in[0,t_{\rm f}]$*, and* $\forall j\in\mathbb{N}_0$*, where* $D(x)\in\mathbb{R}^{m\times m}$ *is the decoupling matrix; then*

$$\lim_{j\to+\infty}\left\|u_{\rm d}(t)-u_j(t)\right\|_\lambda\leq b_{\rm u}\in\mathbb{R}_+\setminus\{+\infty\}\,, \tag{10}$$

$$\lim_{j\to+\infty}\left\|x_{\rm d}(t)-x_j(t)\right\|_\lambda\leq b_{\rm x}\in\mathbb{R}_+\setminus\{+\infty\}\,, \tag{11}$$

$$\lim_{j\to+\infty}\left\|{}^r e_j(t)\right\|_\lambda\leq b_{\rm e}\in\mathbb{R}_+\setminus\{+\infty\}\,. \tag{12}$$

Proof. For the sake of space, we omit the time dependencies. Given (7), defining $\delta u\triangleq u_{\rm d}-u$, $\delta x\triangleq x_{\rm d}-x$, and $\Phi(x,x_{\rm d})\triangleq\sum_{i=0}^{r}{}^i\Upsilon\left(L_f^i h(x_{\rm d})-L_f^i h(x)\right)$, we can compute

$$\begin{aligned}&\delta u_{j+1}+\Gamma_{{\rm fb}_{j+1}}{}^r\Upsilon D(x_{j+1})\delta u_{j+1}=\left(I_m-\Gamma_{{\rm ff}_j}{}^r\Upsilon D(x_j)\right)\delta u_j\\ &-\Gamma_{{\rm fb}_{j+1}}\left(\Phi(x_{j+1},x_{\rm d})-\sum_{i=0}^{r}{}^i\Upsilon w_{j+1}^{(i)}-{}^r\Upsilon\left(D(x_{\rm d})-D(x_{j+1})\right)u_{\rm d}\right)\\ &-\Gamma_{{\rm ff}_j}\left(\Phi(x_j,x_{\rm d})-\sum_{i=0}^{r}{}^i\Upsilon w_j^{(i)}-{}^r\Upsilon\left(D(x_{\rm d})-D(x_j)\right)u_{\rm d}\right)\,.\end{aligned} \tag{13}$$

Recalling assumptions A2 and A3, one has

$$\left|\left|\Phi(x,x_{\mathrm{d}})\right|\right| = \left|\left| \sum_{i=0}^{r} {}^{i}\Upsilon \left(L_f^i h(x_{\mathrm{d}}) - L_f^i h(x)\right) \right|\right| \leq \overline{\phi}\, ||\delta x|| \ , \quad (14)$$

with $\overline{\phi} \geq (r+1)\max\{\left|\left|{}^{0}\Upsilon\phi_0\right|\right|, \cdots, ||{}^{r}\Upsilon\phi_r||\} \geq 0$, and similarly, recalling assumption A5, we compute $\overline{b}_{\mathrm{w}} \geq (r+1)\max\{\left|\left|{}^{0}\Upsilon\right|\right| b_{\mathrm{w1}}, \cdots, ||{}^{r}\Upsilon||\, b_{\mathrm{wr}}\} \geq 0$. Then, starting from (13), we write the following inequalities

$$\begin{aligned}
&\left|\left|I_m + \Gamma_{\mathrm{fb}_{j+1}} {}^{r}\Upsilon D(x_{j+1})\right|\right| \left|\left|\delta u_{j+1}\right|\right| \\
&\leq \left|\left|\Gamma_{\mathrm{fb}_{j+1}}\right|\right| \overline{\phi}\, \left|\left|\delta x_{j+1}\right|\right| + \left|\left|I_m - \Gamma_{\mathrm{ff}_j} {}^{r}\Upsilon D(x_j)\right|\right| \left|\left|\delta u_j\right|\right| \\
&+ \left|\left|\Gamma_{\mathrm{fb}_{j+1}}\right|\right| D_0 \, ||{}^{r}\Upsilon||\, ||u_{\mathrm{d}}||\, \left|\left|\delta x_{j+1}\right|\right| + \left(\left|\left|\Gamma_{\mathrm{fb}_{j+1}}\right|\right| + \left|\left|\Gamma_{\mathrm{ff}_j}\right|\right|\right) \overline{b}_{\mathrm{w}} \\
&+ \left|\left|\Gamma_{\mathrm{ff}_j}\right|\right| \overline{\phi}\, \left|\left|\delta x_j\right|\right| + \left|\left|\Gamma_{\mathrm{ff}_j}\right|\right| D_0 \, ||{}^{r}\Upsilon||\, ||u_{\mathrm{d}}||\, \left|\left|\delta x_j\right|\right| \ .
\end{aligned} \quad (15)$$

Defining $b_\Gamma \triangleq \sup_t\{\max\{\left|\left|\Gamma_{\mathrm{ff}_j}\right|\right|, \left|\left|\Gamma_{\mathrm{fb}_{j+1}}\right|\right|\}\}$, $\mu \triangleq \sup_t \left\{b_\Gamma(\overline{\phi} + D_0\, ||{}^{r}\Upsilon||\, ||u_{\mathrm{d}}||)\right\}$, and $b_{\mathrm{z}} \triangleq \sup_t \left\{\left|\left|\Gamma_{\mathrm{ff}_j}\right|\right| + \left|\left|\Gamma_{\mathrm{fb}_{j+1}}\right|\right|\right\} \overline{b}_{\mathrm{w}}$, and recalling the converge condition (9), (15) can be written as

$$\left|\left|\delta u_{j+1}\right|\right| \leq \rho_{\mathrm{fb}} \left(\mu \left(\left|\left|\delta x_{j+1}\right|\right| + \left|\left|\delta x_j\right|\right|\right) + \rho_{\mathrm{ff}} \left|\left|\delta u_j\right|\right| + b_{\mathrm{z}}\right) \ . \quad (16)$$

Given assumptions A3 and A5, we can write the following inequality for the system (2)

$$\begin{aligned}
\left|\left|\delta x_j\right|\right| \leq b_{\mathrm{l}} &+ \int_0^t \left(f_0 + g_0\, ||u_{\mathrm{d}}(z)||\right) \left|\left|\delta x_j(z)\right|\right| \mathrm{d}z \\
&+ \int_0^t \left|\left|g(x_j(z))\right|\right| \left|\left|\delta u_j(z)\right|\right| + b_{\mathrm{v}} \mathrm{d}z \ .
\end{aligned} \quad (17)$$

Applying the Gronwall's Lemma to (17), leads to

$$\left|\left|\delta x_j\right|\right| \leq b_{\mathrm{l}} \mathrm{e}^{c_2 t} + \int_0^t \left(c_1 \left|\left|\delta u_j(z)\right|\right| + b_{\mathrm{v}}\right) \mathrm{e}^{c_2(t-\tau)} \mathrm{d}z \ , \quad (18)$$

where $c_2 \triangleq \sup_t \{f_0 + g_0\, ||u_{\mathrm{d}}||\}$, and $c_1 \triangleq \sup_t \{||g(x)||\}$. Substituting (18) into (16), computing the $\lambda-$norm, and solving the integrals lead to

$$\begin{aligned}
\left|\left|\delta u_{j+1}\right|\right|_\lambda \leq &\rho_{\mathrm{fb}} \nu \left|\left|\delta u_{j+1}\right|\right|_\lambda \\
&+ \rho_{\mathrm{fb}} \left((\rho_{\mathrm{ff}} + \nu) \left|\left|\delta u_j\right|\right|_\lambda + b_{\mathrm{v}}\right) \ ,
\end{aligned} \quad (19)$$

where $\nu \triangleq \mu c_1 (1 - \mathrm{e}^{(c_2-\lambda)t_{\mathrm{f}}})/(\lambda - c_2)$, and $b_{\mathrm{v}} \triangleq (\mu c_1 + \mu c_1) b_{\mathrm{l}} + b_{\mathrm{z}} + b_{\mathrm{v}} 2\nu$. Defining $\overline{\rho}_{\mathrm{fb}} \triangleq \rho_{\mathrm{fb}}/(1 - \rho_{\mathrm{fb}}\nu)$ and $\overline{\rho}_{\mathrm{ff}} \triangleq (\rho_{\mathrm{ff}} + \nu)$, (19) becomes

$$\left|\left|\delta u_{j+1}\right|\right|_\lambda \leq \overline{\rho}_{\mathrm{fb}} \left(\overline{\rho}_{\mathrm{ff}} \left|\left|\delta u_j\right|\right|_\lambda + b_{\mathrm{v}}\right) \ . \quad (20)$$

Recalling (9), we remark that, $\forall j \in \mathbb{N}_0$, $\forall c_2 \geq 0$, $\exists \lambda \geq 0$ such that $\overline{\rho}_{\mathrm{fb}} < 1$ and $\overline{\rho}_{\mathrm{ff}} < 1$.

Substituting j trials into (20) leads to

$$\left|\left|\delta u_{j+1}\right|\right|_\lambda \leq \overline{\rho}_{\mathrm{fb}}^{j} \overline{\rho}_{\mathrm{ff}}^{j} ||\delta u_0||_\lambda + \overline{\rho}_{\mathrm{fb}} \overline{b}_{\mathrm{v}} \frac{1 - (\overline{\rho}_{\mathrm{fb}} \overline{\rho}_{\mathrm{ff}})^j}{1 - \overline{\rho}_{\mathrm{ff}} \overline{\rho}_{\mathrm{fb}}} \ , \quad (21)$$

where $\overline{b}_{\mathrm{v}} = \max_j\{b_{\mathrm{v}_j}\}$. Computing the limit yields to

$$\lim_{j \to +\infty} \left|\left|\delta u_{j+1}\right|\right|_\lambda \leq \overline{\rho}_{\mathrm{fb}} \overline{b}_{\mathrm{v}} / \left(1 - \overline{\rho}_{\mathrm{ff}} \overline{\rho}_{\mathrm{fb}}\right) \triangleq b_{\mathrm{u}} \ . \quad (22)$$

This proves (10), which is the first thesis of Theorem 1.

To prove (11), we recall (18) and compute its $\lambda-$norm

$$||\, \delta x_j\, ||_\lambda \leq b_{\mathrm{l}} + (c_1\, ||\, \delta u_j\, ||_\lambda + b_{\mathrm{v}}) \nu(\lambda) \ , \quad (23)$$

where, as usual, $\nu(\lambda) = \mu c_1 (1 - \mathrm{e}^{(c_2-\lambda)t_{\mathrm{f}}})/(\lambda - c_2)$. Finally, computing the limit yields to

$$\lim_{j \to +\infty} ||\, \delta x_j\, ||_\lambda \leq b_{\mathrm{l}} + (c_1 b_{\mathrm{u}} + b_{\mathrm{v}}) \nu(\lambda) \triangleq b_{\mathrm{x}} \ . \quad (24)$$

This proves (11), which is the second thesis of Theorem 1.

To prove (12), we rearrange (8) as ${}^{r}e_j = \Phi(x_{\mathrm{d}}, x_j) + D(x_{\mathrm{d}})(u_{\mathrm{d}} - u_j) + (D(x_{\mathrm{d}}) - D(x_j))(u_{\mathrm{d}} - u_j) + (D(x_{\mathrm{d}}) - D(x_j))\, u_{\mathrm{d}}$. Computing its norm yields to

$$\left|\left|{}^{r}e_j\right|\right| \leq \left(\overline{\phi} + D_0 \left|\left|\delta u_j\right|\right| + D_0\, ||u_{\mathrm{d}}||\right) \left|\left|\delta x_j\right|\right| + ||D(x_{\mathrm{d}})||\, \left|\left|\delta u_j\right|\right| \ , \quad (25)$$

Substituting j trials into (25), and computing the limit $j \to +\infty$ leads to

$$\lim_{j \to +\infty} \left|\left|{}^{r}e_j\right|\right| \leq \left(\overline{\phi} + D_0 \left(b_{\mathrm{u}} + ||u_{\mathrm{d}}||\right)\right) b_{\mathrm{x}} + ||D(x_{\mathrm{d}})||\, b_{\mathrm{u}} \triangleq b_{\mathrm{e}} \ , \quad (26)$$

which is (12). The proof of Theorem 1 is completed. □

Remark 1. *The system has a partial relative degree $r < 2n$, thus a Zero Dynamic evolution is present (see, e.g., [19]). However, Theorem 1 claims the $\lambda-$norm boundedness of the whole state, meaning that the Zero Dynamics evolution is bounded too.*

Remark 2. *The feedback convergence condition in* (9) *only requires choosing the proper sign for the gain $\Gamma_{\mathrm{fb}_{j+1}}(t)$.*

C. Stability Analysis of the Equilibrium

In this section, we investigate the stability of the equilibrium $\overline{x} = \left[\overline{q}^{\top}, 0_{n\times 1}^{\top}\right]^{\top}$, and $\overline{u}$. To this end, we linearize the system (2)-(3) in $\overline{x}$ and $\overline{u}$, i.e., $\dot{\xi} = A\xi + B\omega$, $\varsigma = C\xi$, where $\xi \triangleq x - \overline{x}$, $\omega \triangleq u - \overline{u}$, $\varsigma \triangleq y - C\overline{x}$, and the matrices $A \in \mathbb{R}^{2n\times 2n}$, $B \in \mathbb{R}^{2n\times m}$, and $C \in \mathbb{R}^{m\times 2n}$ are

$$\dot{\xi} = \begin{bmatrix} 0_n & I_n \\ -A_{21} & -A_{22} \end{bmatrix} \xi + \begin{bmatrix} 0_{n\times m} \\ B_2 \end{bmatrix} \omega \, , \varsigma = \begin{bmatrix} C_1 & 0_{m\times n} \end{bmatrix} \xi \ , \quad (27)$$

$$\begin{aligned}
&A_{21} = M^{-1}(q) \left(\frac{\partial G(q)}{\partial q} + K\right)\Big|_{\overline{q}}, \quad A_{22} = M^{-1}(\overline{q}) F \ , \\
&B_2 = M^{-1}(\overline{q}) S \, , \quad C_1 = \frac{\partial h(q)}{\partial q}\Big|_{\overline{q}} \ .
\end{aligned} \quad (28)$$

The following Remark proposes a design solution to tackle the stability property of the equilibrium.

Remark 3. *Let us consider the system* (27)*. If the matrix $A_{21} \succ 0$, then A is Hurwitz. This implies that the system* (2) *is locally asymptotically stable in $\overline{x}$ thanks to the Lyapunov indirect Theorem. From* (28)*, we note that A_{21} depends on the system dynamic parameters, e.g., masses, inertias, and stiffness. Then, it is possible to use the Gershgorin circle Theorem to properly design the system in order to guarantee the stability of the equilibrium, in particular satisfying*

$$K_{ii} + \frac{\partial G_i(q)}{\partial q_i} > \sum_{s=1, s\neq i}^{n} \left|\frac{\partial G_i(q)}{\partial q_s}\right| ; \quad \forall i = 1, \cdots, n \ . \quad (29)$$

Despite the observations in Remark 3, A_{21} is likely to be not definite. In this case, we can use the feedback controller to stabilize the equilibrium point. Since $m < 2n$, a common practice is the (dynamic) output feedback, but these methods do not always guarantee stability. For instance, the arbitrary

pole assignment problem can be solved if the condition $(r+1)m \geq 2n$ is verified [21]. However, this is not the case for the system under analysis (27). Conversely, using the controller (7), we can assign $rm < 2n$ eigenvalues, but, generally there is no *a-priori* mathematical guarantee on the (equilibrium) stability, and *a-posteriori* analysis are required [22]. It is worth noting that this is a limit of the presented method.

To study the stabilization problem, we separate the state variables of the linear system (27) applying a complete change of variables $E \in \mathbb{R}^{2n\times 2n}$ such as $E = \begin{bmatrix} C^\top & \dots & (CA^{r-1})^\top & E_1^\top \end{bmatrix}^\top$ with $\text{rank}\{E\} = 2n$ and $E_1 \in \mathbb{R}^{2n-rm\times 2n}$, $\text{rank}\{E_1\} = 2n-rm$. This leads to

$$\begin{cases} \dot{\zeta} = \mathscr{A}\zeta + \mathscr{L}\alpha + \mathscr{B}_1\omega & (30) \\ \dot{\alpha} = \mathscr{Q}\zeta + \mathscr{P}\alpha + \mathscr{B}_2\omega\,, & (31) \end{cases}$$

with $\mathscr{A} \in \mathbb{R}^{rm\times rm}$, $\mathscr{B}_1 \in \mathbb{R}^{rm\times m}$, $\mathscr{L} \in \mathbb{R}^{rm\times 2n-rm}$, $\mathscr{Q} \in \mathbb{R}^{2n-rm\times rm}$, $\mathscr{P} \in \mathbb{R}^{2n-rm\times 2n-rm}$, and $\mathscr{B}_2 \in \mathbb{R}^{2n-rm\times m}$. $\zeta \in \mathbb{R}^{rm}$ describes the part of (27) whose eigenvalues can be assigned via (7), while $\alpha \in \mathbb{R}^{2n-rm}$ belongs to the Zero Dynamics (see, e.g., [19]).

To properly tackle the stabilization problem we introduce the following assumption.

Assumption 6. *The unstable eigenvalues of* (27) *are at most rm. Additionally, they belong to* $\mathscr{A}$ *in* (30).

Note that the stability of the Zero Dynamics can then be guaranteed through design solutions, i.e., Remark 3.

D. Learning Gain Choice

Achieving all the goals listed in Sec. II can be obtained through robot design and a proper choice of the control gains $\Gamma_{\text{fb}_{j+1}}$ and Γ_{ff_j}, $\forall j \in \mathbb{N}_0$. To this end, the following Theorem proposes a possible gain selection method.

Theorem 2. *Let us consider a system in the form* (2)-(3)*, under the assumptions A1-A6. Let us consider the control law* (7) *and the error definition* (8)*. If we choose the learning gains* $\Gamma_{\text{fb}_{j+1}} \in \mathbb{R}^{m\times m}$ *and* $\Gamma_{\text{ff}_j} \in \mathbb{R}^{m\times m}$ *such as*

$$\Gamma_{\text{fb}_{j+1}}(t) = D^{-1}(x_{j+1})\,, \quad \Gamma_{\text{ff}_j}(t) = (1-\varepsilon)D^{-1}(x_j)\,{}^r\Upsilon^{-1}\,, \tag{32}$$

$\forall j \in \mathbb{N}_0\,, \forall t \in [0, t_\text{f}]\,, \varepsilon \in [0,1)$*, where* $D(x) \in \mathbb{R}^{m\times m}$ *is the decoupling matrix; then we claim the following statements.*

- *C1) The equilibrium* $\bar{x} = \left[\bar{q}^\top, 0_{n\times 1}^\top\right]^\top$ *and* $\bar{u}$ *is asymptotically stable for the system* (2)*.*
- *C2) The converge condition* (9) *is fulfilled.*
- *C3) The feedback control law does not alter the robot elastic behavior more than* $\beta \geq 0$*. Additionally,* $\forall \beta \in [0, +\infty)\,, \exists \overline{\phi} \in [0, +\infty)$ *such that* (6) *is valid.*

Proof. To keep the notation clear, we omit the time and iteration dependence. Additionally, let us define the matrix $P(x) \triangleq I_m + \Gamma_{\text{fb}}\,{}^r\Upsilon D(x)$ with $\text{rank}\{P(x)\} = m$, $\forall x \in \mathbb{R}^{2n}$.

First, we prove the statement C1). Recalling assumption A6, the Zero Dynamics evolution is stable by design. On the other hand, the system evolution can be stabilized though the feedback control (7). Recalling that the constant decoupling matrix is $D = CA^{r-1}B$, the linear feedback control is

$$u_\text{fb} = \omega = -P^{-1}\Gamma_\text{fb}\sum_{i=0}^{r} {}^i\Upsilon CA^i\xi\,. \tag{33}$$

Applying (33), we can assign mr eigenvalues in (30), achieving C1).

Second, we prove the statement C2). Note that we explicit the iteration dependence. Assumption A2 guarantees the existence of $D^{-1}(x_j)$, $\forall x \in \mathbb{R}^{2n}$ $\forall j \in \mathbb{N}_0$. Then, we directly substitute (32) into (9) to prove C2).

Finally, we prove the claim C3). Recalling (7), (8), the matrix $P(x)$, and after algebraic manipulation, one has

$$u_\text{fb} = P^{-1}\Gamma_\text{fb}\left(\sum_{i=0}^{r} {}^i\Upsilon\left(L_f^i h(x_\text{d}) - L_f^i h(x)\right) + {}^r\Upsilon D(x_\text{d})u_\text{d}\right), \tag{34}$$

Recalling assumption A2 and substituting (14) and (32) into (34), we can write

$$\begin{aligned} ||\partial u_\text{fb}(\cdot)/\partial q|| \leq \left|\left|\partial D^{-1}(x)/\partial q\right|\right| \left(\overline{\phi}\,||\delta x|| \right. \\ \left. + ||D(x_\text{d})u_\text{d}||\right) + \left|\left|D^{-1}(x)\right|\right|\overline{\phi}\,, \end{aligned} \tag{35}$$

where $\partial D^{-1}(x)/\partial q \triangleq \sum_{i=1}^{n} \partial D^{-1}(x)/\partial q_i$. Recalling (24), assumptions A2, and A3, (35) becomes

$$||\partial u_\text{fb}(\cdot)/\partial q|| \leq 1/\overline{D}_0\left(\overline{\phi}b_\text{x} + \overline{\phi} + ||D(x_\text{d})u_\text{d}||\right) \leq \beta\,, \tag{36}$$

with $1/\overline{D}_0 = \max\{\left|\left|\partial D^{-1}(x)/\partial q\right|\right|, \left|\left|D^{-1}(x)\right|\right|\}$, $\overline{\phi} \geq (r+1)\max\{\left|\left|{}^0\Upsilon\phi_0\right|\right|, \cdots, ||{}^r\Upsilon\phi_r||\}$, and b_x as (24) in Theorem 1.Thus, $\forall\beta \geq 0\,, \forall\,||D(x_\text{d})u_\text{d}||\,, \exists\overline{\phi} \geq 0$, which fulfills (36). □

Remark 4. *Eq.* (32) *requires the knowledge of the whole state, which is not trivial since* $m < 2n$*. However, dealing with Lagrangian systems* (1)*, the decoupling matrix* $D(x)$ *relies on the inertial property of the robot, i.e.,* $r = 2$*. Thus, recalling that* $\exists\varphi_1, \varphi_2 \in \mathbb{R}_+\setminus\{+\infty\}$ *constant and* $v \in \mathbb{R}^n$ *such that* $\varphi_1\,||v|| \leq v^\top M(q)v \leq ||v||\,\varphi_2$*,* (32) *can be written without an accurate knowledge of* $M(q)$ *in* (1) *and the whole robot state, e.g.,* $\forall j \in \mathbb{N}_0$*, and* $\varepsilon \in [0,1)$*, one has* $\Gamma_{\text{fb}_{j+1}} = 1/\varphi_2 I_m$ *and* $\Gamma_{\text{ff}_j} = ((1-\varepsilon)/\varphi_2)\,{}^r\Upsilon^{-1}$*.*

IV. Validation

We validate the proposed algorithm on a two and three DoFs underactuated compliant robots (Fig. 1). This robot is composed of elastic joints, where the first one is actuated and the other are passive, i.e., $m = 1$. The effectiveness of the method is validated both in simulations and on real hardware.

The employed output function (3) is the angular position of the tip of the robot, i.e.,

$$y(t) = h(x(t)) = 1_{1\times n}q\,, \tag{37}$$

which leads to a decoupling matrix such as

$$D(x) = L_g L_f h(x) = 1_{1\times n}M^{-1}(q)S\,. \tag{38}$$

Recalling assumption A2, (38) is full rank $\forall x \in \mathbb{R}^{2n}$, i.e., the system has a fixed relative degree $r = 2$ [18]. The desired trajectory is a minimum jerk signal, which can move the arm

from the initial point $y_\mathrm{i} = 0$ to the final vertical configuration $y_\mathrm{f} = \pi$, i.e., defining $t_\mathrm{s} \triangleq t/t_\mathrm{f}$ one has

$$y_\mathrm{d}(t) = y_\mathrm{i} + (y_\mathrm{i} - y_\mathrm{f}) \left(-10t_\mathrm{s}^3 + 15t_\mathrm{s}^4 - 6t_\mathrm{s}^5\right). \quad (39)$$

In each test, the initial configuration is $x_j(0) = 0_{2n\times 1}\ \forall j \in \mathbb{N}_0$, which is an asymptotically stable equilibrium.

To quantify the tracking performance, we employ the Root Mean Square (RMS) error.

The employed control gains are computed applying Theorem 2 with $\varepsilon = 0.9$. This value was chosen as a trade-off between ILC learning rate and stability, and it allows to fulfill the convergence condition (9) in Theorem 1. Recalling (36), we set $\beta = 2$, so that the variation of the closed-loop elasticity is (in norm) no more than doubled w.r.t. the open-loop one. Tab. I summarizes the selected control gains (${}^i\Upsilon$ for $i = 0, \cdots, r$) for the performed simulations and experiments.

TABLE I
SIMULATIONS AND EXPERIMENTS CONTROL GAINS $\left[{}^0\Upsilon, {}^1\Upsilon, {}^2\Upsilon\right]$

Sim.	DoFs	t_f	Feedback	Feedforward
	3	5s	$[200, 40, 1]$	$[50, 5, 1]$
	2	3s,5s	$[200, 40, 1]$	$[50, 5, 1]$

Exp.	DoFs	t_f	m_2	θ_s	Feedback	Feedforward
	2	5s	0.25kg	20°	$[20, 5, 0.1]$	$[50, 20, 0.5]$
	2	3s	0.25kg	20°	$[100, 30, 0.1]$	$[50, 5, 0.1]$
	2	5s	0.35kg	20°	$[30, 5, 0.1]$	$[100, 30, 0.5]$
	2	3s	0.35kg	20°	$[20, 5, 0.1]$	$[30, 10, 0.1]$
	2	5s	0.35kg	16°	$[30, 20, 0.5]$	$[20, 20, 1]$
	2	3s	0.35kg	16°	$[20, 10, 0.1]$	$[20, 10, 0.1]$

A. Simulation Results

We tested the effectiveness of the methods simulating two robots: 2 and 3 DoFs arms. The parameters of the employed model are: mass $m_i = 0.55$kg, inertia $J_{i,i} = 0.01$kgm^2, length $l_i = 0.089$m, center of mass distance $a_i = 0.085$m, damping coefficient $F_{i,i} = 0.1$Nms/rad, and stiffness $K_{i,i} = 1$Nm/rad for $i = 1, 2, 3$. These parameters are used for both simulating robot dynamics and to compute the learning gains.

Defining $\sqrt{\mathrm{i}} \triangleq -1$ and computing the linear model (27) leads to open-loop eigenvalues equal to $-\left\{7 \pm 6.5\mathrm{i} \quad 3.4 \quad -2.1\right\}$ for the 2 DoFs arm, and equal to $-\left\{2.4 \quad 3 \quad -3.2 \quad 5.2 \quad 31 \quad 83\right\}$ for the 3 DoFs arm. This means that the vertical equilibrium of both systems is unstable due to the presence of a real positive eigenvalue. However, the control law (33) can stabilize the vertical equilibrium since $1 < rm$. Applying Theorem 2, we choose the control gains Υ as in Tab. I, obtaining closed-loop eigenvalues equal to $-\left\{49 \quad 9 \quad 0.22 \pm 3\mathrm{i}\right\}$ and $-\left\{2.0 \pm 0.67\mathrm{i} \quad 3 \quad 9.7 \quad 27 \pm 65\mathrm{i}\right\}$, respectively, i.e., we stabilize the equilibrium point.

1) 3 DoFs Simulation Results: We test the method on the 3 DoFs arm described in Sec. IV-A, with a null initial guess and performing (39) with $t_\mathrm{f} = 5$s.

Fig.2 reports the results. Fig.2(a) shows the error evolution over iterations. Fig.2(b)-2(c) depict the final tracking performance and joints evolution, respectively.

2) 2 DoFs Simulation Results: To validate the learning capabilities of the method, we perform several simulations varying the initial guess $u_0(t)$, noise, and uncertainties. In all the cases the reference trajectory is the minimum jerk signal (39) with $t_\mathrm{f} = 5$s. We test three different initial guess designs: (i) $u_0(t) \equiv 0$, (ii) Reference (R)-like, and (iii) Computed Torque (CT)-like. The design (ii) is computed as $u_0(t) = K_{1,1} y_\mathrm{d}(t)$, and it is thought to be an (almost) model-free method to design an initial guess.

Conversely, method (iii) is model-based. Generally, it is not trivial to compute a model-based initial guess for the class of systems under analysis, because they are underactuated, i.e., $m = 1$ and $n = 2$. Indeed, this leads to the existence of infinite solutions of (3) choosing (37). For this reason, the CT-like initial guess is computed assuming that $q_1^{(i)}(t) = y_\mathrm{d}^{(i)}(t)$ and $q_2^{(i)}(t) \equiv 0$ for $i = 0, 1, 2$. Recalling (1)-(4), the CT-like action is

$$u_0 = \left(M_{1,1} - M_{1,2}M_{2,2}^{-1}M_{2,1}\right)\ddot{q}_{\mathrm{d}_1} + N_1 - M_{1,2}M_{2,2}^{-1}N_2\,. \quad (40)$$

Additionally, all the simulations are also performed injecting white noise with zero mean and standard deviation 0.03. Furthermore, in the case of the CT-like (40) initial guess (with and without noise), we also perturb the nominal parameters via multiplicative uncertainty randomly picked in $[0.75, 1.25]$, performing a total of 50 different simulations. It is worth highlighting that these uncertainties affect both the initial guess (40) and the learning gains (32).

Fig.3 reports all the simulations results. Fig. 3(a) shows the error evolution over iterations, Fig.3(b) reports the final tracking performance, Fig. 3(c)) shows the different initial guesses, and Fig. 3(d)) depicts the control actions at the last iteration ($j = 15$).

B. Experimental Results

The experimental setup is depicted in Fig. 1 in which the elastic actuation is obtained with qb-Move Advanced [23]. This is a variable stiffness actuator with elastic torque $\tau_\mathrm{e} = 2\iota\cosh(\kappa\theta_\mathrm{s})\sinh(\kappa(q_i - \theta_\mathrm{e}))$ and nonlinear stiffness function $\sigma = 2\kappa\iota\cosh(\kappa\theta_\mathrm{s})\cosh(\kappa(q_i - \theta_\mathrm{e}))$, where $\kappa = 6.7328\mathrm{rad}^{-1}$, and $\iota = 0.0222$Nm. θ_s tunes the desired stiffness profile, and during the experiments, it is set constant. θ_e is the motor equilibrium position, and, assuming negligible motor dynamics, it can be considered the control input instead of τ in (1). It is worth mentioning that, even if θ_s is set constant, the actual stiffness profile σ is nonlinear and depends on the deflection. This introduces a modeling error in the experiments. As second link, we employ again a qbMove Advanced actuator, but we do not actuate it and we set θ_s constant and θ_e null. This pragmatic solution allows us to have a passive joint equipped with a torsional spring and a position encoder sensor.

The validation is performed with (39) as reference trajectory, using two different final times, i.e., $t_\mathrm{f} = 5$s and $t_\mathrm{f} = 3$s. Additionally, we test two stiffness scenarios: the Stiff one with $\theta_\mathrm{s} = 20°$, leading to $K_{i,i} = 1.57$Nm/rad ($i = 1, 2$) in (1), and the Soft one with $\theta_\mathrm{s} = 16°$ and $K_{i,i} = 1$Nm/rad. Furthermore, we also vary the payload, testing $m_2 = 0.25$kg and $m_2 = 0.35$kg. In total, we perform six experiments varying payload, trajectory velocity, and stiffness profile. Simulations are also reported for comparison.

In open-loop, the vertical equilibrium is not stable, while using the feedback controller (7) with the control parameters

This article has been accepted for publication in a future issue of this journal, but has not been fully edited. Content may change prior to final publication. Citation information: DOI 10.1109/LRA.2022.3144786, IEEE Robotics and Automation Letters

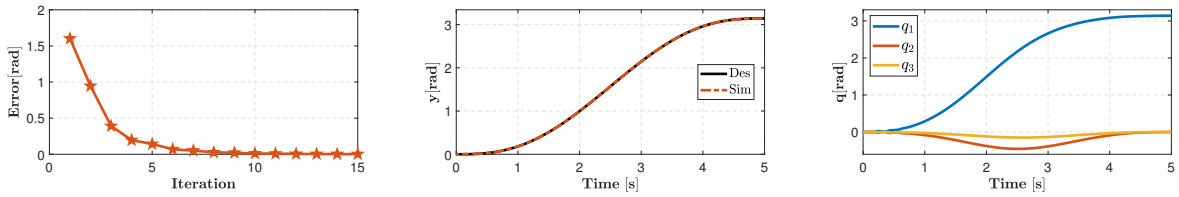

(a) Error evolution over iteration. (b) Output tracking performance. (c) Output tracking performance.

Fig. 2. Simulation results for 3 DoFs robot in the case of trajectory executed in $t_f = 5$s.

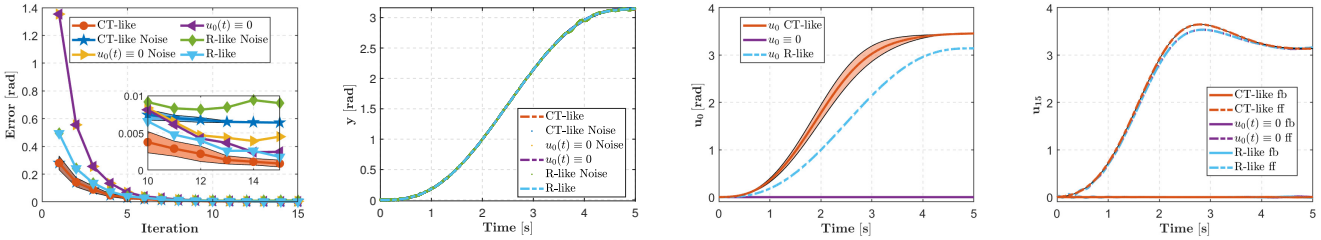

(a) Error evolution over iteration. (b) Output tracking performance. (c) Initial guess u_0. (d) Final control u_{15}.

Fig. 3. Simulation results for the case of trajectory executed in $t_f = 5$s.

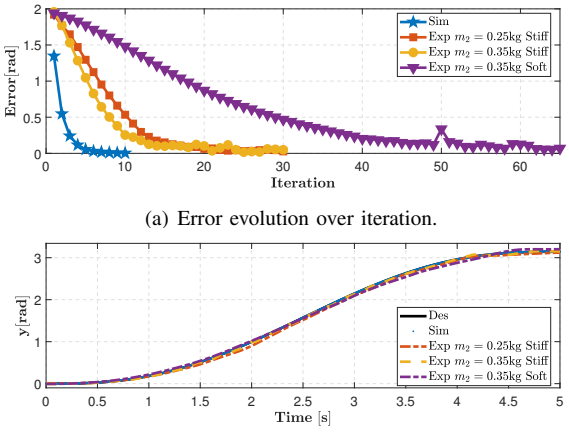

(a) Error evolution over iteration.

(b) Output tracking performance.

Fig. 4. Simulation and experimental results for $t_f = 5$s.

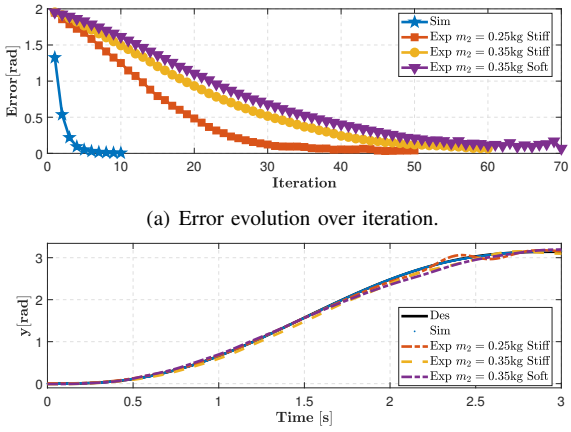

(a) Error evolution over iteration.

(b) Output tracking performance.

Fig. 5. Simulation and experimental results for $t_f = 3$s.

in Tab. I, we obtain a stable closed-loop behavior. It is worth highlighting that the model used during the experiments and the velocity measurements are not accurate. This affects also the estimation of the decoupling matrix (38).

Fig.4-5 report both the simulations and experimental results for $t_f = 5$s and $t_f = 3$s, respectively. Fig.4(a)-5(a) show the error evolution over iterations. Fig.4(b)-5(b) report the tracking performance at the last iteration. Finally, Fig.6 shows the photo-sequence of the experiment case for $t_f = 5$s. Please refer to the video attachment.

C. Discussion

Results show that the proposed control algorithm is able to learn the desired trajectory, swinging-up the underactuated compliant arm varying the number of DoFs, stiffness, payload, disturbances, and velocities, Fig. 2(b)-3(b)-4(b)-5(b). As supported by the system analysis, the feedback component is able to stabilize the system in the vertical configuration. This can be achieved because only one eigenvalue lies in the real positive plane. It is worth noting that, despite the presence of

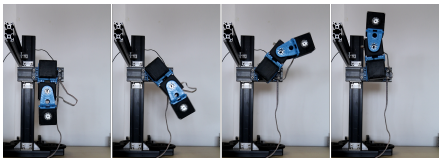

Fig. 6. Photo-sequence of the experimental tracking with $t_f = 5$s.

the feedback, the variation of closed-loop stiffness is small thanks to Proposition 1 and Theorem 2. Indeed, the stiffness variation averaged among all the experiments is ∼0.65Nm/rad. Additionally, at the last iteration, the control action is almost exclusively feedforward (Fig. 3(d)), confirming the stiffness preservation.

As shown by Fig. 3(a), different choices of initial guess modify the tracking performance at the first iteration. In particular, we have that better designs (Fig. 3(c)) greatly reduce this error, and improve the learning rate. However, at the end of the learning phase, the achieved performances are (almost) equal (Fig. 3(b)). Indeed, also the learned control inputs are (almost) equal (Fig.3(d)).

The presence of uncertainties affects both the initial guess design (40) and the learning gains (32). Nevertheless, the proposed method achieves good tracking performance (Fig. 3). However, as claimed by Theorem 1, in presence of noisy data, the learning rate is slower, and the method converges to a bounded value Fig. 3(a). These observations hold true also in the experiments Fig.4-5, where uncertainties and noise are due to the inaccuracy of the model and of the sensors.

Fig. 4(a)-5(a) show that the learning rate is faster in simulation employing only 10 iterations to convergence. Note also that in simulation the feedback allows also to improve the performance in the initial trial ($j = 1$) because the gains are greater (Tab. I). However, at the end of the learning phase, the performances are satisfying in all the scenarios. In particular, in the simulations, thanks to the accuracy of the model and measurements, the method achieves a final averaged RMS error equal to $\sim$0.003rad, while the experimental RMS error averaged in all cases is $\sim$0.03rad.

As shown by Fig. 2(c) and by the attached video, the underactuation of the robot causes a non-negligible motion of the passive links. However, the method is able to achieve the desired vertical configuration Fig. 2(b)-3(b)-4(b)-5(b).

Various conditions have been tested in the experiments. From these results, we noticed that the cases with $t_{\mathrm{f}} = 3$s are the most challenging, leading to a slower learning rate Fig. 4(a)-5(a). Additionally, we have that the learning rate is affected mainly by the joint stiffness rather than the payload. However, the tracking performances are comparable in all the scenarios Fig. 4(b)-5(b).

V. Conclusion and Future Work

In this letter, we presented an Iterative Learning Control framework for underactuated compliant arms performing trajectory tracking with a particular focus on swing-up tasks. The proposed iterative controller merges feedforward and feedback terms without requiring any accurate robot model. The robot reaches the vertical configuration tracking the desired trajectory with good performance thanks to the feedforward component. On the other hand, the feedback term guarantees the stability of the vertical equilibrium point. A condition on the feedback gain avoids any drastic alteration of robot elasticity, allowing the preservation of the system compliance. The convergence of the iterative algorithm is proved even in presence of model uncertainties and measurements noise. The effectiveness of the proposed approach is tested through simulations and on real hardware varying number of DoFs, initial guess, disturbances, system compliance, payload, and trajectory velocity.

Future work will mainly focus on tackling the main limitations of the proposed approach. In particular, relaxing assumptions A2 and A6, i.e., relative degree dependence and Zero Dynamics evolution, respectively. Furthermore, at the moment the method relies on output feedback, thus it can stabilize systems presenting only $rm < 2n$ unstable eigenvalues. Finally, we will extend the proposed control algorithm to continuum soft robots [14], [24].

References

[1] M. W. Spong, "Partial feedback linearization of underactuated mechanical systems," in *Proceedings of IEEE/RSJ International Conference on Intelligent Robots and Systems (IROS'94)*, vol. 1. IEEE, 1994, pp. 314–321.

[2] X. Xin *et al.*, "Energy-based swing-up control for a remotely driven acrobot: Theoretical and experimental results," *IEEE Transactions on Control Systems Technology*, vol. 20, no. 4, pp. 1048–1056, 2011.

[3] A. Cristofaro *et al.*, "Linear-quadratic optimal boundary control of a one-link flexible arm," *IEEE Control Systems Letters*, vol. 5, no. 3, pp. 833–838, 2020.

[4] G. Turrisi *et al.*, "Enforcing constraints over learned policies via nonlinear mpc: Application to the pendubot."

[5] X. Q. Ma *et al.*, "A new fuzzy approach for swing up control of pendubot," in *Proceedings of the 2002 American Control Conference (IEEE Cat. No. CH37301)*, vol. 2. IEEE, 2002, pp. 1001–1006.

[6] A. Kukker *et al.*, "Genetic algorithm-optimized fuzzy lyapunov reinforcement learning for nonlinear systems," *Arabian Journal for Science and Engineering*, vol. 45, no. 3, pp. 1629–1638, 2020.

[7] S. Gillen *et al.*, "Combining deep reinforcement learning and local control for the acrobot swing-up and balance task," in *2020 59th IEEE Conference on Decision and Control (CDC)*. IEEE, 2020, pp. 4129–4134.

[8] A. Verl *et al.*, *Soft Robotics*. Springer, 2015.

[9] D. Rus *et al.*, "Design, fabrication and control of soft robots," *Nature*, vol. 521, no. 7553, pp. 467–475, 2015.

[10] T. M. Bieze *et al.*, "Fem-based kinematics and closed-loop control of soft, continuum manipulators."

[11] C. Della Santina *et al.*, "Controlling soft robots: balancing feedback and feedforward elements," *IEEE Robotics & Automation Magazine*, vol. 24, no. 3, pp. 75–83, 2017.

[12] F. Angelini *et al.*, "Decentralized trajectory tracking control for soft robots interacting with the environment," *IEEE Transactions on Robotics*, vol. 34, no. 4, pp. 924–935, 2018.

[13] T. G. Thuruthel *et al.*, "Learning dynamic models for open loop predictive control of soft robotic manipulators," *Bioinspiration & biomimetics*, vol. 12, no. 6, p. 066003, 2017.

[14] C. Della Santina *et al.*, "Dynamic control of soft robots interacting with the environment," in *2018 IEEE International Conference on Soft Robotics (RoboSoft)*. IEEE, 2018, pp. 46–53.

[15] D. Camilleri *et al.*, "Analysing the limitations of deep learning for developmental robotics," in *conference on Biomimetic and Biohybrid Systems*. Springer, 2017, pp. 86–94.

[16] S. Arimoto *et al.*, "Bettering operation of dynamic systems by learning: A new control theory for servomechanism or mechatronics systems," in *The 23rd IEEE Conference on Decision and Control*. IEEE, 1984, pp. 1064–1069.

[17] R. Mengacci *et al.*, "On the motion/stiffness decoupling property of articulated soft robots with application to model-free torque iterative learning control," *The International Journal of Robotics Research*, p. 0278364920943275, 2020.

[18] M. Pierallini *et al.*, "Trajectory tracking of a one-link flexible arm via iterative learning control," in *2020 IEEE/RSJ International Conference on Intelligent Robots and Systems (IROS)*. IEEE, 2020, pp. 7579–7586.

[19] A. Isidori, *Nonlinear Control Systems Design 1989: Selected Papers from the IFAC Symposium, Capri, Italy, 14-16 June 1989*. Elsevier, 2014.

[20] H.-S. Ahn *et al.*, "Iterative learning control for a class of nonlinear systems," *Automatica*, vol. 29, no. 6, pp. 1575–1578, 1993.

[21] J. Rosenthal *et al.*, "Output feedback pole placement with dynamic compensators," *IEEE Transactions on Automatic Control*, vol. 41, no. 6, pp. 830–843, 1996.

[22] A. Andry *et al.*, "Eigenstructure assignment for linear systems," *IEEE transactions on aerospace and electronic systems*, no. 5, pp. 711–729, 1983.

[23] R. Mengacci *et al.*, "Overcoming the torque/stiffness range tradeoff in antagonistic variable stiffness actuators," *IEEE/ASME Transactions on Mechatronics*, 2021.

[24] L. Cenceschi *et al.*, "Pi σ-pi σ continuous iterative learning control for nonlinear systems with arbitrary relative degree," in *2021 European Control Conference (ECC)*. IEEE, 2021.